Aerospace Engineering Communications
http://dx.doi.org/10.62762/AEC.2026.303859

RESEARCH ARTICLE

Advanced Barrier Function-Based Robust Prescribed Performance Control with Actuator Fault

Xiaoyu Zhu[1,*], **Ran Sun**[2], **Jihe Wang**[3] **and Pukun Lu**[4]

[1] School of Aeronautics and Astronautics, Shanghai Jiao Tong University, Shanghai 200240, China
[2] School of Optical-Electrical and Computer Engineering, University of Shanghai for Science and Technology, Shanghai 200093, China
[3] School of Aeronautics and Astronautics, Sun Yat-Sen University (Shenzhen Campus), Shenzhen 518107, China
[4] Department of Earth and Space Science and Engineering, York University, Toronto, ON M3J 1P3, Canada

Abstract

This paper investigates prescribed performance control (PPC) using an advanced barrier function (ABF) based adaptive super-twisting control scheme with non-fragility. The specialty of the proposed scheme is that it removes the error transformation process, and therefore simplifies the design of PPC. Furthermore, the ABF is combined with an online adaptation law to solve the problem of fragility inherent to the traditional PPC. The proposed method is robust to actuator faults, unknown initial states, and sudden disturbances. The stability of the system is proved via the Lyapunov framework. Finally, experiments on a two-degree-of-freedom (2-DOF) helicopter platform are conducted to verify the effectiveness of the control strategy.

Keywords: advanced barrier function, prescribed performance, super-twisting control.

Submitted: 28 March 2026
Accepted: 19 April 2026
Published: 22 April 2026

Vol. 1, **No.** 2, 2026.
10.62762/AEC.2026.303859

***Corresponding author:**
✉ Xiaoyu Zhu
xiaoyuzhu@sjtu.edu.cn

1 Introduction

For industrial control with matching transient and steady-state indicators, prescribed performance control (PPC) has shown its high efficiency [1]. Indeed, it provides a convenient way to determine the tracking error evolution process in advance. The objective of PPC is to guarantee the system trajectory to stay within the performance envelope. With wide engineering applications, such as autonomous rendezvous under motion constraints [2, 3], flight safety, and collision avoidance [4, 5], researchers pay increased attention to ensuring the system's transient performance.

However, PPC requires the knowledge of initial states, faults, and disturbances, which could be conservative from a practical point of view. In the control process, it is often inevitable to exceed the performance function envelope caused by unknown initial states, actuator faults, and sudden disturbances, which highlights the need for disturbance-free and high-precision control architectures [6]. So, many researchers focus on avoiding the fragility associated with the traditional PPC. More importantly, the prescribed performance constraint, introduced by Bechlioulis and Rovithakis in [1], is hard to satisfy in the controller directly. Thus,

Citation
Zhu, X., Sun, R., Wang, J., & Lu, P. (2026). Advanced Barrier Function-Based Robust Prescribed Performance Control with Actuator Fault. *Aerospace Engineering Communications*, 1(2), 68–80.

they need to utilize a new error transformation to guarantee the prescribed tracking performance, which results in a more complex design.

1.1 Related works

Robust prescribed performance control (RPPC) was proposed against dynamic uncertainties, unknown system uncertainties, external disturbances, and variable parameters, which makes it easy to be extended to multiple-input multiple-output (MIMO) nonlinear systems [1]. Benefiting from the improvements, RPPC provides an efficient way to achieve high-quality control for feedback systems [7]. In [8], RPPC was applied to guarantee the desired performance for spacecraft attitude tracking, despite unknown but constant inertia parameters, external disturbances, actuator faults, and input saturation. Additionally, adaptive learning observers [9], fixed-time disturbance observers [10], and advanced composite state observers [11, 12] have been effectively utilized to handle actuator faults and non-fragile tracking in spacecraft control. Then, they applied the RPPC to a spacecraft pose tracking with a freely tumbling target [13]. The results show the efficiency of RPPC in MIMO systems. In [14], a learning-based two-layer prescribed performance attitude control approach for spacecraft formation was investigated to solve the coordinated attitude tracking problem. For multi-spacecraft missions, prescribed performance attitude control has been extensively studied under various constraints [15], and advanced model predictive control architectures have been developed for formation flying [16]. Additionally, adaptive dynamic event-based robust control has been investigated for multiple networked systems [17]. Meanwhile, dynamic event-triggered reinforcement learning [18], attention-driven reinforcement learning [19], and reinforced Lyapunov controllers [20] have been successfully applied to multi-satellite collaborative tracking and robust trajectory maneuver scheduling [21]. Similarly, self-learning [22] and online-learning [23] control frameworks have been developed to further enhance attitude tracking precision. In [24], a modal-disturbance observer was proposed to handle the impact of unexpected disturbances caused by flexible vibrations on the PPC. In [25], a neural network-based PPC for 2-DOF helicopter system was introduced to deal with system uncertainties. Similarly, adaptive neural dynamic-based control strategies have shown efficiency in stabilizing complex aerospace systems [26], and decentralized inverse neural control frameworks have been established for complex interconnected systems [27].

However, the above methods assume that the system states must be within the performance envelope. They do not solve the fragility of existing PPC [28]. It may suffer singularity when the expected state constraint is violated [29]. For example, most performance functions can not deal with the unknown initial state. The hyperbolic cotangent performance function seems to solve the problem [30], but setting the initial parameter of the performance function to infinity sacrifices the transient indicators of the system, which is contrary to the original intention of PPC. Lei et al. [31] proposed a singularity-avoidance PPC scheme with a reference performance function. However, they must assume that the disturbance is bounded. But, commonly, the system's state does not meet the performance constraints when sudden faults or disturbances occur [32]. For this point, Bu et al. [33] proposed a new type of non-fragile prescribed performance function containing readjusting terms to deal with actuator saturation. The proposed method can self-adjust its prescribed funnel, and successfully remedy the fragility defect associated with the existing PPC.

Another issue is that the controller cannot directly implement the performance constraint in the existing PPC. Instead, an error transformation framework is utilized to guarantee that [34]. However, using the error transformation framework makes the controller design process complicated. In [35–39], monitoring and barrier functions (MBF) are proposed for the design of PPC. Owing to the dynamic properties of MBF, the requirement for the error transformation is removed, and the barrier function confines the output within a small prescribed vicinity of the origin. However, MBF is a switching scheme, which results in a discontinuous state of the system. In their results, the tracking trajectory has an obvious jump at the switching point.

1.2 Contribution and outline

In this paper, we propose an advanced barrier function-based prescribed performance control (ABFPPC) with non-fragility, subject to actuator faults, unknown initial states, and sudden disturbances. The main contributions of this paper are:

1) Compared with the traditional PPC [40, 41] framework, the prescribed performance constraint can be directly satisfied in the controller without the need of error transformation. In turn, the

control design is simpler and no longer needs the transformed error.

2) Compared with MBFPPC [35], which uses a combination of monitoring function and barrier function to implement PPC, the modification in the ABF replaces the monitoring function part, which leads to a more compact form. Meanwhile, the chattering problem caused by the monitoring function's switching scheme is avoided.

3) An adaptive strategy is designed to deal with the fragile problem associated with the traditional PPC [40, 41], improving the robustness of the controller.

These theoretical advancements directly translate to practical engineering advantages. By avoiding the complex error transformation and singularity issues, the proposed ABFPPC significantly reduces the computational burden and parameter tuning effort, making it highly suitable for real-time aerospace applications under unpredictable environments.

This paper is organized as follows. Section 2 presents the problem formulation. The controller design and the proof are given in Section 3. Experimental studies are conducted in Section 4. Finally, we conclude our work in Section 5.

2 Problem Formulation

Consider the following system given by

$$\dot{x}_1 = x_2 \tag{1}$$
$$\dot{x}_2 = h(t)u(t) + d(t) \tag{2}$$

where $x = [x_1, x_2] \in \mathbb{R}^2$, $u \in \mathbb{R}$ is the control variable, $h \in \mathbb{R}$ and $d \in \mathbb{R}$ are unknown bounded fault and unknown disturbance.

Assumption 1 *The derivative of disturbance $d(t)$ is assumed to be bounded by unknown boundary*

$$|\dot{d}(t)| \leq \tilde{d}_{\max} \tag{3}$$

where $\tilde{d}_{\max} > 0$ is unknown constants.

Assumption 2 *The actuator fault $h(t)$ is bounded with unknown boundary, satisfying*

$$h_{\min} \leq |h(t)| \leq h_{\max}, \tag{4}$$

where $h_{\min} > 0$ and $h_{\max} > 0$ are unknown constant.

2.1 Prescribed performance

For standard prescribed performance [34], the tracking error $e_1(t) = x_1(t) - x_{1,d}(t)$ should converge to a predefined arbitrarily small residual set, with convergence rate no less than a certain pre-specified value, i.e.,

$$-\eta(t) < e_1(t) < \eta(t) \tag{5}$$

where $\eta(t)$ is exponentially decaying function with: $\eta(0) = \varphi > 0$ and $-\dot{\eta}(t) \leq c\eta(t),\ c > 0$. Usually $\eta(t) = (\eta_0 - \eta_\infty)\exp(-lt) + \eta_\infty$ is chosen as the performance function, given by

$$\eta(t) = (\eta_0 - \eta_\infty)\exp(-lt) + \eta_\infty \tag{6}$$

where $\eta_0 > 0$, $\eta_\infty > 0$ and $l > 0$ are constants.

2.2 Advanced barrier function

Motivated by the barrier function in [37–39], which showed the potential to achieve PPC-like behavior, the ABF is defined as follows.

Definition 1. Suppose that there is a η as in (6), $K^*_\beta : x \in (-\eta, \eta) \to K^*_\beta(x) \in [\beta, \infty)$ strictly increase on $[0, \eta)$, in which $K^*_\beta(x)$ satisfies $K^*_\beta(0) = \beta > 0$ and $\lim_{|x| \to \eta} K_\beta(x) = +\infty$, with

$$K^*_\beta(\eta(t), x) = \frac{\sqrt{\eta(t)}\beta}{\sqrt{\eta(t) - |x|}} \tag{7}$$

3 Controller Design

In this section, the ABFPPC with non-fragility is presented. First, we will illustrate the details of using ABF (7) to achieve PPC without error transformation. Second, a special adaptation for super-twisting control is designed to avoid the fragility.

3.1 Advanced barrier function-based PPC

Define a sliding variable

$$s = e_2 + \lambda e_1 \tag{8}$$

where $e_1 = x_1 - x_{1,d}$ and $e_2 = x_2 - x_{2,d}$ are the tracking errors, λ is a positive constant. Then, the control $u = u_s$ is given as

$$u_s = -K^*_\beta(\eta(t), s)\langle s(t)\rangle^{1/2} + u_{s,2} - \lambda\dot{e}_1 + \dot{x}_{2,d} \tag{9}$$
$$\dot{u}_{s,2} = -K^{*2}_\beta(\eta(t), s)\langle s(t)\rangle^0 \tag{10}$$

where the notation $\langle x\rangle^\alpha$, denote $|x|^\alpha \operatorname{sign}(x)$, $x, \alpha \in \mathbb{R}$.

Theorem 1 *Consider system (1)-(2) with control law (9)-(10) and a non-increasing prescribed performance* *function* $\eta(t) = (\eta_0 - \eta_\infty)\exp(-lt) + \eta_\infty$*, Then, for all* $t \geq 0$*, one has* $|s(t)| \leq \eta(t)$*. Moreover,* e_1 *and* e_2 *will still converge to a small residual set,* $\lim_{t\to\infty} |e_1(t)| \leq \eta_\infty/\lambda$*,* $\lim_{t\to\infty} |e_2(t)| \leq 2\eta_\infty$*.*

Proof. Taking derivative of s in (8) with $\dot{e}_2 = \dot{x}_2 - \dot{x}_{2,d}$ as mentioned above, we have

$$\dot{s} = \dot{e}_2 + \lambda\dot{e}_1 = (hu_s + d - \dot{x}_{2,d}) + \lambda\dot{e}_1 \tag{11}$$

Substituting (9) into (11), one can obtain

$$\begin{aligned} \dot{s} &= -hK_\beta^*(\eta(t), s)\langle s(t)\rangle^{1/2} + hu_{s,2} \\ &\quad - h\lambda\dot{e}_1 + h\dot{x}_{2,d} + d - \dot{x}_{2,d} + \lambda\dot{e}_1 \\ &= h[-K_\beta^*(\eta(t), s)\langle s(t)\rangle^{1/2} + u_{s,2}] \\ &\quad + h[\frac{h-1}{h}(\dot{x}_{2,d} - \lambda\dot{e}_1) + \frac{d}{h}] \end{aligned} \tag{12}$$

Defining the lumped disturbance $D(t)$ and the auxiliary variable $\Psi(t)$ as

$$D(t) = \frac{h-1}{h}(\dot{x}_{2,d} - \lambda\dot{e}_1) + \frac{d}{h} \tag{13}$$

$$\Psi(t) = u_{s,2} + D(t) \tag{14}$$

Then, the dynamics of the system can be rewritten as

$$\dot{s}(t) = h[-K_\beta^*(\eta(t), s)\langle s(t)\rangle^{1/2} + \Psi(t)] \tag{15}$$

$$\dot{\Psi}(t) = -K_\beta^{*2}(\eta(t), s)\langle s(t)\rangle^{0} + \dot{D}(t) \tag{16}$$

According to Assumptions 1 and 2, $\dot{D} \leq \tilde{D}_{\max}$ is bounded by an unknown boundary. The remaining proof process can be divided into two steps.

Step 1: When $t \geq 0$, we need to prove that $|s(t)| \leq \eta(t)$. Define the change of variables $z = (z_1, z_2)$ given by:

$$z_1 = {K_\beta^*}^2 s(t), \ z_2 = \Psi(t) \tag{17}$$

In these variables, the system can be written as follows:

$$\dot{z}_1 = 2\frac{\partial K_\beta^*}{\partial s K_\beta^*} z_1 + {K_\beta^*}^2 \dot{s} \tag{18}$$

$$\dot{z}_2 = \dot{\Psi} \tag{19}$$

where

$$\frac{\partial K_\beta^*}{\partial s} = \frac{\beta\sqrt{\eta}(\eta - |s|)^{1/2}\dot{s}\langle s\rangle}{2(\eta - |s|)} \tag{20}$$

with the initial state satisfies $|z_1(0)| \leq \beta^2\eta_0$.

Substituting (20) into the term $\partial K_\beta^*/\partial s K_\beta^*$ is given as

$$\frac{\partial K_\beta^*}{\partial s K_\beta^*} = \frac{1/2\ \dot{s}\langle s\rangle^0}{(\eta - |s|)} = C_\eta {K_\beta^*}^2 \dot{s}\langle s\rangle^0 \tag{21}$$

where $C_\eta = 1/(2\beta^2\eta)$.

To clearly show the derivation of the simplified dynamics, we substitute (21) into the first equation of (18):

$$\begin{aligned} \dot{z}_1 &= 2\left(C_\eta {K_\beta^*}^2 \dot{s}\langle s\rangle^0\right) z_1 + {K_\beta^*}^2 \dot{s} \\ &= {K_\beta^*}^2 \dot{s}\left(1 + 2C_\eta z_1\langle s\rangle^0\right) \end{aligned} \tag{22}$$

Since $z_1 = {K_\beta^*}^2 s$, it holds that $z_1\langle s\rangle^0 = |z_1|$. By defining $G(z) = 1 + 2C_\eta|z_1|$, we obtain:

$$\dot{z}_1 = {K_\beta^*}^2 \dot{s} G(z) \tag{23}$$

Dividing both sides by $G(z)$ and substituting $\dot{s}$ from (15), noting that $\langle z_1\rangle^{1/2} = K_\beta^*\langle s\rangle^{1/2}$ and $z_2 = \Psi$, one obtains:

$$\dot{z}_1/G(z) = K_\beta^{*2} h(-\langle z_1\rangle^{1/2} + z_2) \tag{24}$$

$$\dot{z}_2 = -{K_\beta^*}^2\langle z_1\rangle^0 + \dot{D} \tag{25}$$

Since $\dot{D}$ is bound, whatever the choice of η is, $K_{\beta,i}^* > \beta$ by definition. So, (25) shows that $\dot{z}_2$ is bounded. The design of $u_{s,2}$ is reasonable.

Then, define Lyapunov function V_1 as

$$V_1 = \frac{\ln G(z)}{2C_\eta}\left(1 - \frac{1}{4}\langle z_1\rangle^0\phi(z_2)\right) + \frac{F(z)z_2^2}{2} \tag{26}$$

where $\phi(z_2)$ and $F(z)$ are defined as

$$\phi(z_2) = \langle z_2\rangle^0 \min(|z_2, 1|) \tag{27}$$

$$F(z) = \begin{cases} h_{\min}, \text{ if } \langle z_1\rangle^0 z_2 \leq 0 \\ h_{\max}, \text{ if } \langle z_1\rangle^0 z_2 > 0 \end{cases} \tag{28}$$

The following inequality holds

$$\frac{3\ln G(z)}{8C_\eta} + \frac{h_{\min}z_2^2}{2} \leq V_1 \leq \frac{5\ln G(z)}{8C_\eta} + \frac{h_{\max}z_2^2}{2} \tag{29}$$

Hence, V_1 is positive-definite. Then, the following fact needs to be satisfied

$$\lim_{t\to\infty} V_1 \leq V^* \tag{30}$$

where V^* is a positive constant only depending on $h_{\min}$, $h_{\max}$, and $\tilde{D}_{\max}$.

Taking the derivative of the Lyapunov function (26), one gets

$$\begin{aligned} \dot{V}_1 &= \frac{\dot{z}_1\langle z_1\rangle^0}{G} + F\dot{z}_2 z_2 - \frac{\dot{z}_1\phi(z_2)}{4G} - \frac{\dot{\phi}(z_2)\langle z_1\rangle^0 \ln G}{8C_\eta} \\ &\leq -\frac{1}{2}|z_1|^{\frac{1}{2}} - |z_2|\left(\frac{1}{4} - \frac{\tilde{D}_{\max}}{\beta^2 G}\right) + \dot{\phi}(z_2)\frac{\tilde{D}_{\max}}{8\beta^2 C_\eta}\frac{\ln G}{G} \end{aligned} \tag{31}$$

Define

$$V^* = 8(1 + h_{\max}^2 + \frac{1}{h_{\min}^2})C_D^2 + \frac{5\ln 1 + 2C_\eta z_D}{C_\eta}(1 + \frac{1}{h_{\min}}) \tag{32}$$

where $C_D = \tilde{D}_{\max}/\beta$ and $z_D = 4(C_D - 1/8)/C_\eta$.

We can prove by contradiction: there exists an increasing sequence of times $t_n, n \geq 0$ tending to infinity such that

$$V_1(t_n) \leq \frac{V^*}{2} \tag{33}$$

If (33) does not hold, there exists $t_0 \geq 0$ such that one has, for $t \geq t_0 V_1 \geq V^*/2$. Moreover, if any trajectory of (15) is in the strip at some time $t \geq t_0$ then it must go through it in time cross verifying

$$t_{\text{cross}} \leq \frac{2\ln(1+4C_D)}{h_{\min} z_2} \leq \frac{\ln(1+4C_D)}{C_D} \tag{34}$$

Reference [39] claims that the trajectory of (15) must enter into the strip. Indeed, otherwise

$$\dot{V}_1 \leq -\frac{1}{2}|z_1|^{\frac{1}{2}} - \frac{1}{8}|z_2| \tag{35}$$

A simple examination of the phase portrait in the region $z_1 > z_D$ shows that the trajectory of (15) must enter the region $0 < 2z_2 < z$ it in finite time along the axis $z_2 = 0$. Hence, there exists an interval of time $[t_1, t_2]$ such that

$$\sqrt{z_1}(t_1) = 2z_2(t_1), z_2(t_2) = 0 \tag{36}$$

Then $z_2(t_1) \geq \sqrt{V^2}/2$, $t_2 - t_1 \geq \frac{7}{4}z_2(t_1)$ and

$$-\frac{\langle z_1\rangle^{\frac{1}{2}}}{2} \leq \frac{\dot{z}_1}{G} \leq -\langle z_1\rangle \tag{37}$$

This is impossible and (33) is proved.

Step 2: Define Lyapunov function V_2 as

$$V_2 = \frac{1}{2}e_1^2 \tag{38}$$

Lemma 1 [42] *When the sliding mode vector s designed as in (8) converges to a small set containing the origin (that is $|s| \leq \Delta$, where Δ is a positive constant), then e_1 and e_2 will converge to a small residual set, $e_1 \leq \Delta/\lambda$ and $e_2 \leq 2\Delta$.*

Then, the derivative of V_2 is given by

$$\dot{V}_2 = e_1\dot{e}_1 \tag{39}$$

Substituting Eq. (8) into Eq. (39), we have

$$\begin{aligned}\dot{V}_2 &= e_1(s - \lambda e_1) = -\lambda e_1^2 + se_1 \\ &\leq \|e_1\|\left(-\lambda|e_1| + |s|\right)\end{aligned} \tag{40}$$

From Eq. (40) and Lemma 1, when $t \to \infty$, it is obvious that

$$\lim_{t\to\infty} |e_1(t)| \leq \eta_\infty/\lambda \tag{41}$$

Combining the supposed condition in Theorem 1: $\lim\limits_{t\to\infty} |s(t)| \leq \eta(t)$ with Eq. (41), we have

$$\lim_{t\to\infty}\|e_2(t)\| \leq \lim_{t\to\infty}\|s(t)\| + \lambda\lim_{t\to\infty}\|e_1(t)\| \leq 2\eta_\infty \tag{42}$$

Owing to the decreasing property of $\eta(t)$, e_1 and e_2 are bounded if the defined sliding-mode variable s converges to within a small neighborhood around $s = 0$. The proof of Theorem 1 is complete.

3.2 Non-fragile strategy

Consider system (15) with adaptive parameter $K_\beta^*(\eta(t), s)$, the main problem draws on the case when unknown initial states or sudden disturbances occur, the expected state constraint (5) is violated. Replacing $K_\beta^*(\eta(t), s)$ in (9) with new adaptive parameters $L(t)$ and $M(t)$, the controller can be rewritten as

$$u_s = -L(t)\langle s(t)\rangle^{1/2} + u_{s,2} - \lambda\dot{e}_1 + \dot{x}_{2,d} \tag{43}$$

$$\dot{u}_{s,2} = -L^2(t)\langle s(t)\rangle^0 - M(t)\langle s(t)\rangle^0 \tag{44}$$

where the variable gain $L(t)$ is defined as follows

$$L(t) = \begin{cases} L_1(t - t_a) + L_0, & \text{if } t - t_a < \bar{t}(s_0) \\ K_\beta^*(\eta(t), s), & \text{if } t - t_a \geq \bar{t}(s_0)\end{cases} \tag{45}$$

$$M(t) = \begin{cases} 0, & \text{if } s(t) \geq \eta(t) \\ M_0, & \text{if } s(t) < \eta(t)\end{cases} \tag{46}$$

where L_1, L_0, and M_0 are positive constants, t_a is the time when the sliding-mode variable exceeds $\eta(t)$ considering the case that the controller is subject to unknown initial states and sudden disturbances.

Lemma 2 [36] *Consider system (1)-(2) with adaptive control law in (43)-(45) and a small constant $\varepsilon > 0$, $L_1 > 0$, $L_0 > 0$, for every $s_0 = s(0)$, there exists a first time $\bar{t}(s_0)$, where $|s(t)| \leq \varepsilon/2$. Then, for all $t \geq \bar{t}(s_0)$, one has $|s(t)| \leq \varepsilon$.*

Lemma 3 [38] *Considering an integer system (1)-(2), there exists a law u as follows:*

$$u = g(u_0(|s|))u_0(s) + b\,\text{sign}(u_0(|s|))L(t, V_1(s)) \quad (47)$$

where V_1 is a continuous positive definite function, g is an arbitrary increasing function tending to infinity, u_0 is a feedback controller, b is a positive constant. Then, for every $s_0 = s(0)$, if $t > 0$, there exists a time $\bar{t}(V_1(s_0))$ for which $V_1(s(t)) \leq \eta(t)/2$ at $t = t(V_1(s_0))$ and $s(t)$ for all $t > t(V_1(e_0))$, $V_1(s_0) \leq \eta(t)$, where $\eta(t)$ is a non-increasing function, and satisfies $-\dot{\eta}(t) \leq l\eta(t),\ l > 0$.

According to Lemma 3, replacing the small constant ε in Lemma 2 with a non-increasing function η will not affect system stability. For example, let $u_0 = s$ and $V_1(s(t)) = |s|^{1/2}$, if $g = u_{s,2}$ lead to the boundness of the second equation of (48), then according to the properties of exponential function, $|s| \leq \eta(t)$.

The point is that we need to guarantee that the system solution will reach $\eta(t)/2$ since the condition $\bar{t}(s_0)$ disappears. Here, a simple term $M(t)\langle s(t)\rangle^0$ helps us achieve this.

Lemma 4 [43] *Consider the following motion equations,*

$$\begin{cases} \dot{s} = -a\langle s(t)\rangle^{1/2} + \Psi \\ \dot{\Psi} = -M_0\langle s(t)\rangle^0 + f(t) \end{cases} \quad (48)$$

where $|f(t)| < f_0$, $M_0 > f_0$, f_0 and M_0 are constant positive constants. Define $E = M_0 - f_0$, if $E > 0$, the state convergences to zero after a finite time interval. Moreover, there exists a^*, if $a(t) > a^*$ such that the state is reduced to zero in finite time. The convergence time tends to $s(0)/m$ with $a \to \infty$.

Remark 1 *We do not need to guarantee that $E > 0$ for system (15) as in Lemma 4. The second equation of Eq. (24) shows that $\dot{\Psi}$ is bounded, since $\dot{z}_2$ is bounded with the term $-K_{\beta}^{*2}(\eta(t), s)\langle s(t)\rangle^0$. Therefore, introducing $M(t)$ here does not aim to overcome the disturbance. The main purpose is to speed up the convergence from $\eta(t)$ to $\eta(t)/2$.*

Remark 2 *It is worth noting that if there is no unknown initial state or sudden disturbance, the controller (9) is sufficient to achieve the capabilities of traditional PPC. The variable gain $L_1(t - t_a) + L_0$ in (45) is equivalent to resetting the control strategy of the system on-line. In the following experiments, the controller sometimes cannot provide enough input to overcome sudden disturbance. In this case, the system state will exceed the performance envelope.*

4 Experimental Studies

The proposed controller in (9)-(10) and (43)-(46) will be utilized to control the system. The results of the proposed ABFPPC are compared with the traditional PPC in [40, 41] and MBFPPC in [35].

The experiment will be demonstrated using a 2-DOF helicopter as shown in Figure 1. The Quanser Aero can be configured as a conventional dual-rotor helicopter. The front motor that is horizontal to the ground predominantly affects the motion of the pitch axis, and the back motor mainly affects the motion of the yaw axis. Both the front and back motors generate torque on each other, this is a coupled system.

The system employs a control algorithm that generates control commands in the form of voltage signals to drive the motor. The motor then produces a control torque at the rotor, which regulates the system dynamics. Define (θ, ϕ) the pitch and yaw angles. The sampling rate is selected as 200Hz. The real-time control is realized. The dynamic equations of the input-output behaviors can be expressed as

$$J_p\ddot{\theta} + R_p\dot{\theta} + K_{sp}\theta = h_p(t)u_p + d_p \quad (49)$$

$$J_y\ddot{\varphi} + R_y\dot{\varphi} = h_y(t)u_y + d_y \quad (50)$$

where θ and φ are the pitch angle and the yaw angle expressed in the body frame, $\dot{\theta}$, $\dot{\varphi}$, $\ddot{\theta}$ and $\ddot{\varphi}$ are the corresponding angular velocities and accelerations, u_i, d_i, h_i, J_i and R_i, $i = p, y$ are the control inputs, the external disturbances, the fault characterizing the health conditions of controller, the total moments of inertia and the damping ratio parameter about the pitch and yaw axes, respectively, K_{sp} is the stiffness parameter about the pitch axis.

Without actuator faults, the control inputs are related to the voltages of the pitch and yaw motors and can be expressed as

$$u_p = K_{pp}V_p + K_{py}V_y \quad (51)$$

$$u_y = K_{yp}V_p + K_{yy}V_y \quad (52)$$

where V_p and V_y are the voltages applied to the pitch and yaw motors, respectively, K_{pp} and K_{yy} are the torque thrust parameters of the pitch and yaw motors, respectively, K_{py} is the cross-torque thrust parameter acting on the pitch from the yaw motor, K_{yp} is the cross-torque thrust parameter acting on the yaw from the pitch motor.

To stabilize the 2-DOF helicopter attitude control system, the following sliding variable $\boldsymbol{s} = [s_p, s_y]^{\mathrm{T}}$ is defined:

$$\begin{cases} s_p = \frac{1}{\lambda_p^*}\dot{\theta}_e + \theta_e \\ s_y = \frac{1}{\lambda_y^*}\dot{\varphi}_e + \varphi_e \end{cases} \tag{53}$$

where $\lambda_p^* > 0$ and $\lambda_y^* > 0$.

Then, consider the kinematics and dynamics system (49) and (50), let $\boldsymbol{x}_1 = [\theta_e, \varphi_e]^{\mathrm{T}} = [x_{1p}, x_{1y}]^{\mathrm{T}}$ and $\boldsymbol{x}_2 = \dot{\boldsymbol{x}}_1$. The sliding mode variable can be rewritten as $\boldsymbol{s} = \boldsymbol{x}_2 + \boldsymbol{\lambda}\boldsymbol{x}_1$. Then, we get the state space model of the 2-DOF helicopter [44]

$$\dot{\boldsymbol{x}}_1 = \boldsymbol{x}_2 \tag{54}$$

$$\dot{\boldsymbol{x}}_2 = F(\boldsymbol{x}_1, \boldsymbol{x}_2) + \boldsymbol{H}(t)\boldsymbol{u}(t) + \hat{\boldsymbol{d}}(t) \tag{55}$$

where $F(\boldsymbol{x}_1, \boldsymbol{x}_2) = \begin{bmatrix} -K_{sp}/J_p\, x_{1p} & -R_p/J_p\, x_{1y} \\ 0 & -R_y/J_y\, x_{2y} \end{bmatrix}$, $H(t) = \mathrm{diag}\{h_p/J_p, h_y/J_y\}$, and $\hat{\boldsymbol{d}}(t) = [d_p/J_p\, , d_y/J_y\,]^{\mathrm{T}}$.

During the experiments, the actuators may suffer from unknown faults. The model of the actuator failure model is chosen as in [41]:

$$\boldsymbol{u} = \boldsymbol{K}(t)\boldsymbol{u_s}(t) + \boldsymbol{\Gamma}(t) \tag{56}$$

where $\boldsymbol{u_s}(t)$ is the control input as designed in (9) and (43)-(46). $\boldsymbol{K}(t) = \mathrm{diag}\{k_p(t), k_y(t)\}$ indicates an actuator gain fault with $0 < k_0 < k_i(t) \leq 1, (i = p, y)$ being an effective factor for the ith actuator, where k_0 is a positive constant. $\boldsymbol{\Gamma}(t) = [\gamma_p(t), \gamma_y(t)]^{\mathrm{T}}$ denotes a bounded signal.

Instead of just generating the parameters of actuator faults in Matlab as in [41], the following experimental scenario was adopted as shown in Figure 2. We unlock the connection between the rotor and the body. Then, the rotor is flexible, and the control inputs with actuator faults satisfy

$$u_p = \underbrace{\cos\alpha_p(t)}_{k_p(t)} u_{sp}(t) + \underbrace{\sin\alpha_y(t) u_{sy}(t)}_{\gamma_p(t)} \tag{57}$$

$$u_y = \underbrace{\cos\alpha_y(t)}_{k_y(t)} u_{sy}(t) + \underbrace{\sin\alpha_p(t) u_{sp}(t)}_{\gamma_y(t)} \tag{58}$$

where $0 \leq \alpha_p < \pi/2$ and $0 \leq \alpha_y < \pi/2$. The exact value of α_p and α_y are unknown during the experiment. (57)-(58) physically implemented the description of actuator faults in (56).

Remark 3 *We use the sliding mode variable (53) instead of the sliding mode variable (8) in the experiments. Because such a performance envelope is more intuitive, that is,* $\lim_{t\to\infty} |\theta_e| \leq 2\eta_{p\infty}$, $\lim_{t\to\infty} |\dot{\theta}_e| \leq \lambda_p^*\eta_{p\infty}$, $\lim_{t\to\infty} |\varphi| \leq 2\eta_{y\infty}$, $\lim_{t\to\infty} |\dot{\varphi}| \leq \lambda_y^*\eta_{y\infty}$.

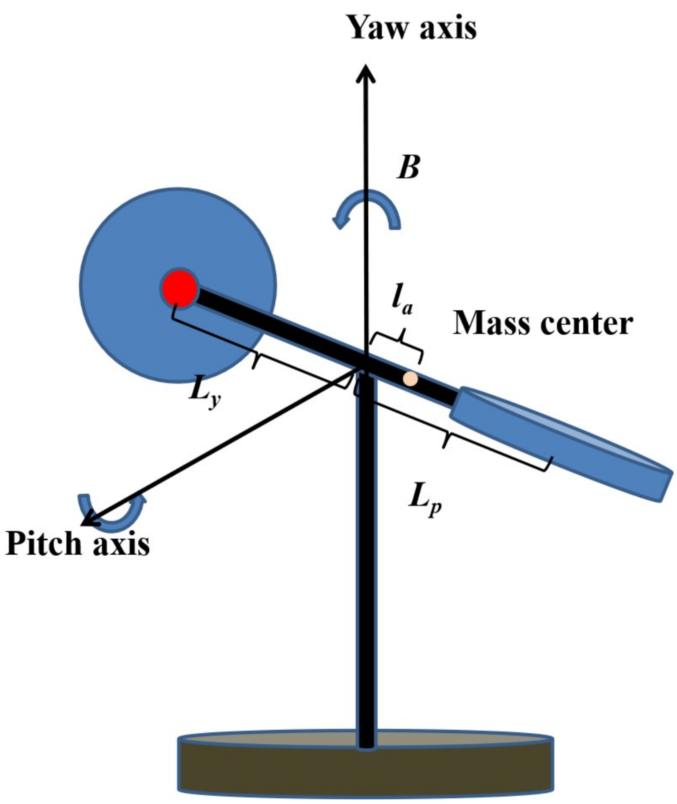

Figure 1. 2-DOF helicopter.

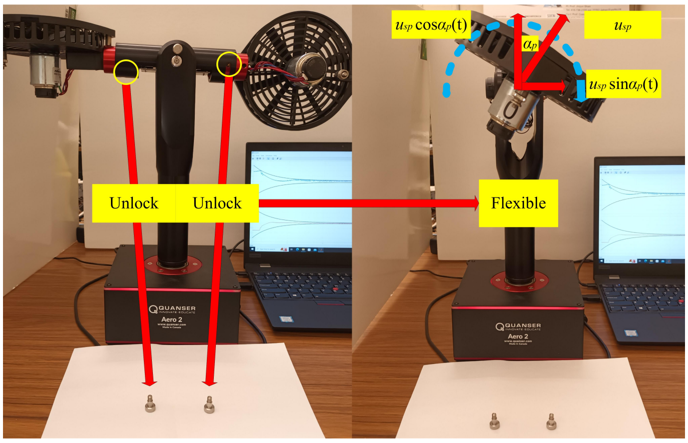

Figure 2. Actuator fault settings for 2-DOF helicopter.

Remark 4 *Since we remove the rivets fixing the helicopter's body, the expected trajectory amplitude cannot be too large, and the movement cannot be too fast, otherwise the helicopter's actuator will fall.*

4.1 Parameter setting

The initial states of the 2-DOF helicopter, the torque thrust parameters of the pitch and yaw motors, and the parameters of the ABFPPC are listed in Table 1. The core parameters of the comparative traditional PPC and MBFPPC are tuned to their optimal values as suggested in [40] and [35], respectively, to ensure a fair comparison. The desired attitude is designed as $\theta_d(t) = (\pi/16)\sin 0.25t + 0.12$ rad and $\varphi_d(t) = (\pi/48)\sin 0.3t - 0.12$ rad. We use the subscripts p and y to distinguish parameters on different axes.

Table 1. Experimental parameters.

2-DOF helicopter	Values	Controller	Values
$\theta_e(0)$(rad)	0.25	L_{p1}	0.02
$\dot{\theta}_e(0)$(rad/s)	0	L_{p0}	0.07
$\varphi_e(0)$(rad)	-0.15	L_{y1}	0.02
$\dot{\varphi}_e(0)$(rad/s)	0	L_{y0}	0.07
m_{body}(kg)	1.0750	λ_p^*	6.25
V_{pmax}(V)	24	λ_y^*	6.25
V_{ymax}(V)	24	M_0	0.05
$J_p(\mathrm{kg \cdot m^2})$	0.0219	β_p	0.07
$J_y(\mathrm{kg \cdot m^2})$	0.0220	β_y	0.07
$\Delta J_p(\mathrm{kg \cdot m^2})$	0.0014	l_p	0.2
$\Delta J_y(\mathrm{kg \cdot m^2})$	0.0009	l_y	0.4
$K_{pp}(\mathrm{N \cdot m/V})$	0.0012	η_{p0}	0.25
$K_{yy}(\mathrm{N \cdot m/V})$	0.0022	η_{y0}	0.2
$K_{py}(\mathrm{N \cdot m/V})$	0.0021	$\eta_{p\infty}$	0.015
$K_{yp}(\mathrm{N \cdot m/V})$	-0.0014	$\eta_{y\infty}$	0.01

4.2 The proposed controller

As shown in Figure 3, the ABFPPC could force the sliding variable $\boldsymbol{s}$ to satisfy the prescribed performance function in the presence of actuator faults. In turn, Figure 4 shows that the output (θ, φ) can follow the desired trajectory (θ_d, φ_d), which meets our control objective. Figures 5 and 6 indicate that the tracking errors of angles and angular velocities also satisfy Theorem 1 and Remark 4: $\lim_{t\to\infty} |\theta_e| \leq 2\eta_{p\infty}$, $\lim_{t\to\infty} |\dot{\theta}_e| \leq 6.25\eta_{p\infty}$, $\lim_{t\to\infty} |\varphi| \leq 2\eta_{y\infty}$, $\lim_{t\to\infty} |\dot{\varphi}| \leq 6.25\eta_{y\infty}$.

Quantitative analysis indicates that the proposed ABFPPC achieves superior steady-state performance. Specifically, the maximum tracking error of the proposed method is reduced by approximately 35% compared to the traditional PPC under standard operating conditions, and the steady-state error is strictly maintained within 0.015 rad, validating its precision and robustness.

Remark 5 *The sliding variable* $\boldsymbol{s}$ *is equivalent to the filtering error in* [40]. [41] *improves* [40] *with fault-tolerant control scheme.*

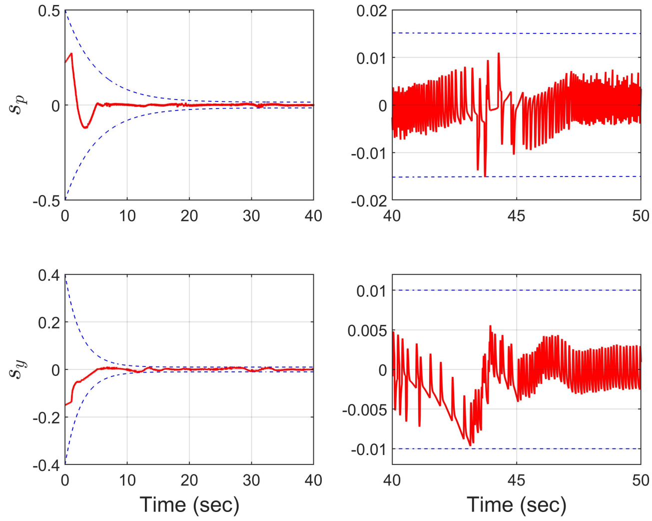

Figure 3. Sliding variables of the proposed method.

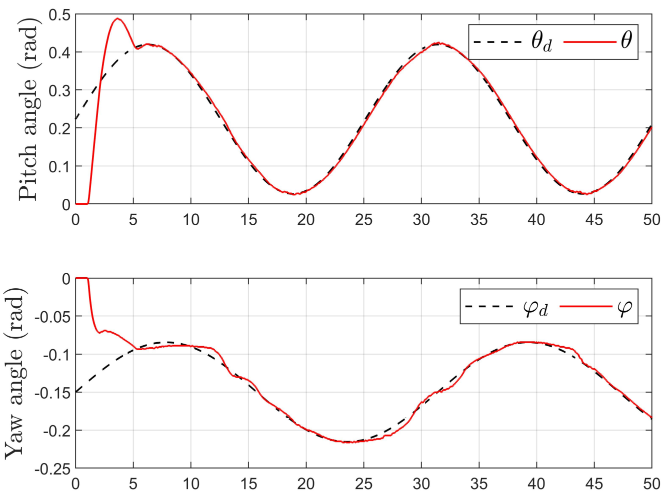

Figure 4. Attitude tracking results.

4.3 Comparison to fault-tolerant control with prescribed performance under sudden disturbances

In this subsection, we want to further verify the stability of the proposed controller under extreme conditions to see if the non-fragile strategy (43)-(46) can improve the system's robustness to sudden disturbance exceeding the controller capability. The results are compared with adaptive neural fault-tolerant control for a 2-DOF helicopter system with prescribed performance in [40, 41]. Researchers assumed the controller could limit the states to the pre-defined envelope of traditional PPC. However, sudden disturbances may exceed the controller's capability in reality.

As shown in the supplementary video (https://youtu.be/mhYPbOSzzdk), the 2-DOF helicopter states escape

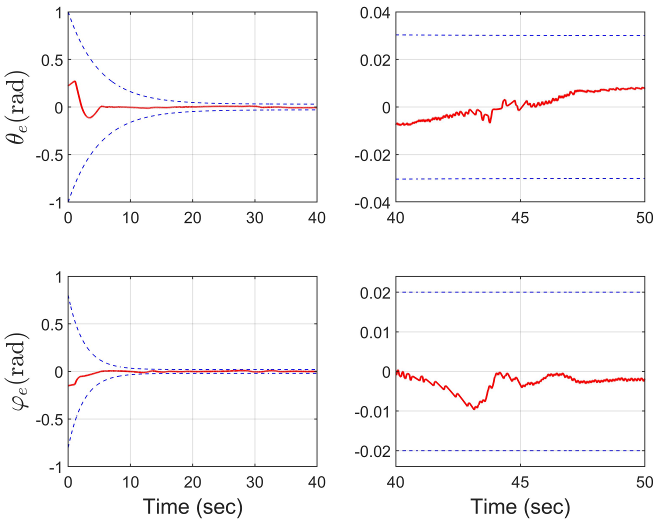

Figure 5. Tracking errors of attitude.

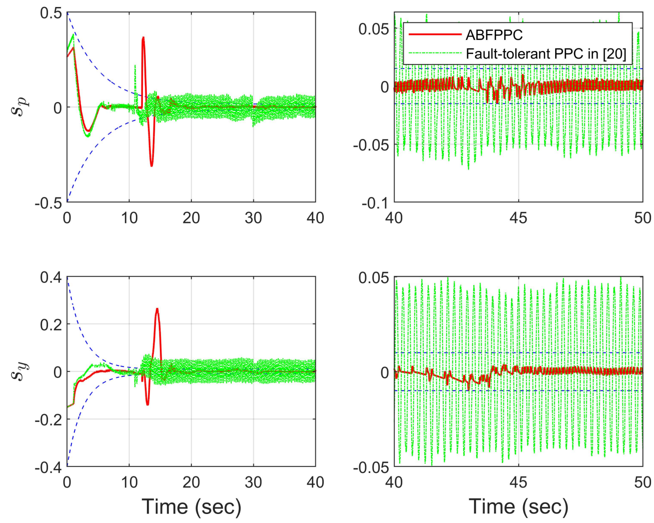

Figure 7. Comparison of sliding variables under sudden disturbances: (a) with ABFPPC, (b) with fault-tolerant PPC in [40].

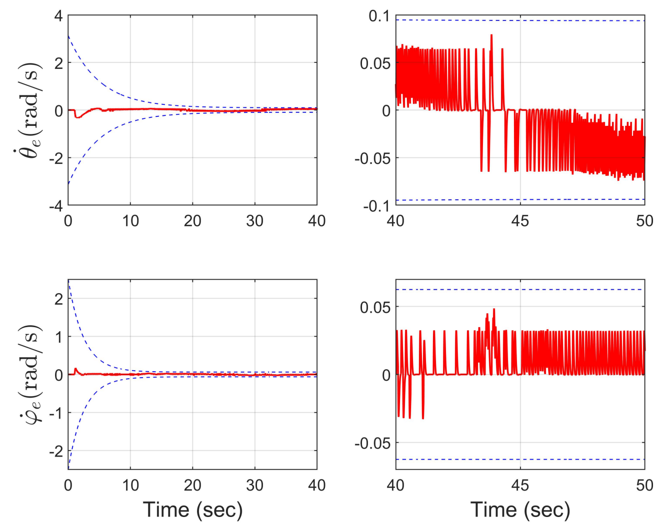

Figure 6. Tracking errors of angular velocities.

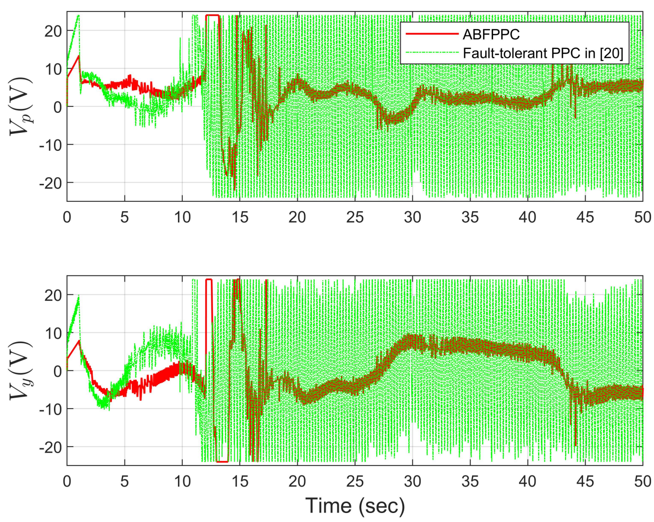

Figure 8. Comparison of control input under sudden disturbances: (a) with ABFPPC, (b) with fault-tolerant PPC in [40].

from the pre-defined envelope by sudden disturbances and faults. The results are shown in Figure 7, and the performance comparisons between the proposed controller and adaptive neural fault-tolerant control with prescribed performance in [40, 41] are presented. We give the 2-DOF helicopter a sudden disturbance and fault at about 12 s, physically injecting the bounded uncertainties defined in Eq. (57) and (58). Their values in the red line (our method) are larger than in the green line (method in [40, 41]). Although the controller of [40, 41] is robust and can cope with a certain degree of external disturbance and actuator fault, once there is a sudden disturbance and fault, the control output deteriorates and becomes saturated as shown in Figure 8. The system states is in vibration and cannot return to the performance envelope. However, the proposed controller can maintain control performance under sudden disturbances. It validates the non-fragility of ABFPPC.

4.4 Comparison to fault-tolerant control with prescribed performance under unknown initial states

In addition to sudden disturbances, we also verified the effectiveness of the controller under unknown initial states. The results are still compared with adaptive neural fault-tolerant control for a 2-DOF helicopter system with prescribed performance in [40, 41]. The initial states are changed to $\theta_e(0) = 0.6$ rad and $\varphi_e(0) = -0.5$ rad.

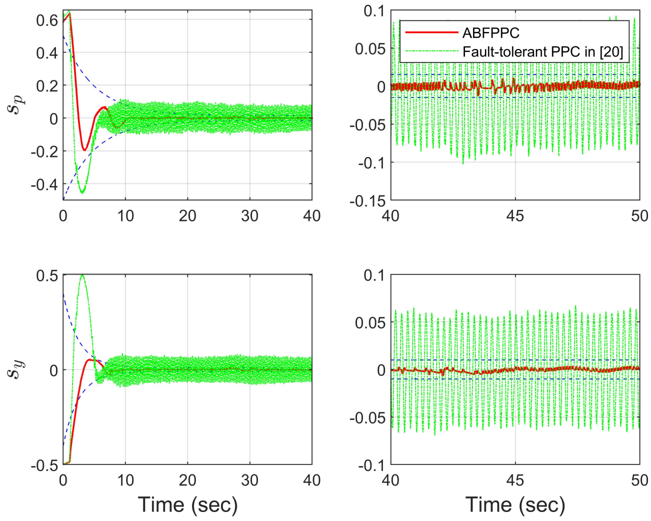

Figure 9. Comparison of sliding variables unknown initial states: (a) with ABFPPC, (b) with fault-tolerant PPC in [40].

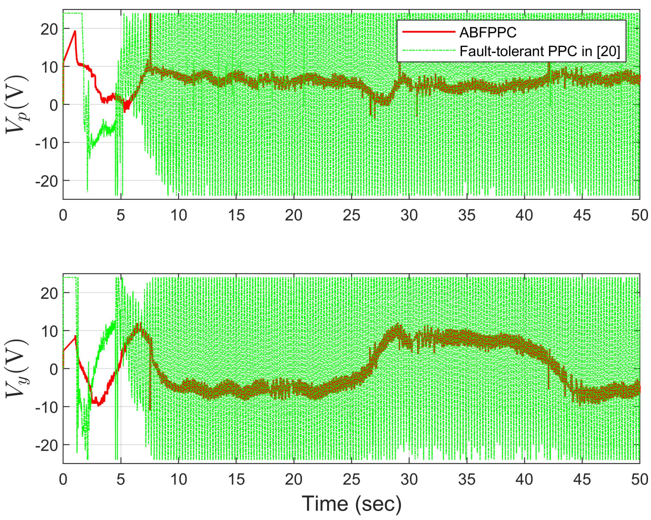

Figure 10. Comparison of control input under unknown initial states: (a) with ABFPPC, (b) with fault-tolerant PPC in [40].

As shown in Figures 9, although the initial system states are out of the envelopes, they still strictly meet the conditions when they enter the performance envelope in the convergence process for the red line. It indicates that the variables can be set out of the performance envelope, and not exceed the envelope again with ABFPPC. On the other hand, [40, 41] fails to restrict the attitude within the performance envelope, once the initial system states are out of the envelopes. The control signals are shown in Figure 10. Compared with [40, 41], our method does not fall into saturation due to unknown initial states.

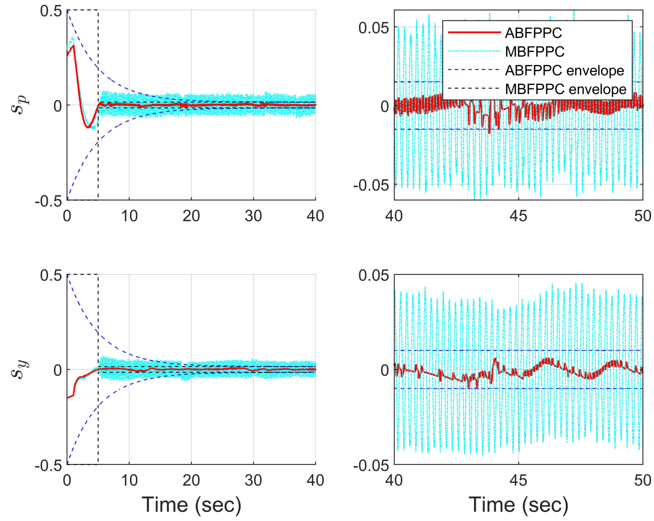

Figure 11. Comparison of sliding variables: (a) with ABFPPC, (b) with MBFPPC in [35].

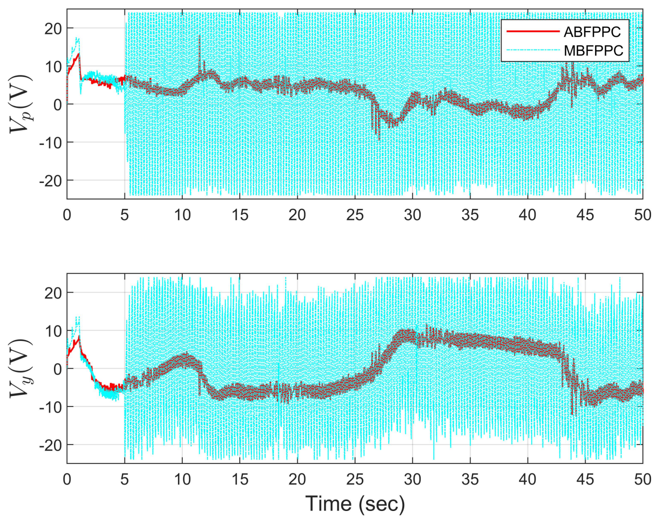

Figure 12. Comparison of control inputs: (a) with ABFPPC, (b) with MBFPPC in [35].

4.5 Comparison to MBFPPC

In this subsection, we compare the performance between the proposed method and MBFPPC in [35]. The results are shown in Figures 11 and 12. Since the monitoring function is an appropriate switching-based scheme, during the convergence process, the system state is discontinuous at the switching point (about 5s), which will lead to chattering in the subsequent process. ABFPPC overcomes this problem and allows the state to smoothly satisfy exponential decrease.

5 Conclusion

In this paper, we study the advanced barrier function-based prescribed performance control with non-fragility, subject to unknown initial states, actuator faults, and sudden disturbances. The advantage of the proposed method is that the states satisfy the performance functions with a specially designed barrier function instead of using transformed error. The performance functions are related to actual performance constraints without changing the control framework. Benefiting from this, a simple adaptation law for ABFPPC is designed to cope with unknown initial states, sudden disturbances, and actuator faults. The experimental results using a 2-DOF helicopter show that the system can achieve the prescribed performance even with robustness and non-fragility.

Compared to traditional methods, the core innovation of completely removing the error transformation while guaranteeing non-fragile stability simplifies the implementation process. Ultimately, the proposed ABFPPC provides a highly reliable, low-complexity, and practically viable solution for complex aerospace engineering missions.

In future work, we will further discuss the relationship between η_∞ and chattering. In the experiment, we find that if η_∞ is too small, regardless of the adaptive method used, PPC control will experience chattering. Therefore, we hope to solve this problem.

Data Availability Statement

Data will be made available on request.

Funding

This work was supported without any funding.

Conflicts of Interest

The authors declare no conflicts of interest.

AI Use Statement

The authors declare that no generative AI was used in the preparation of this manuscript.

Ethical Approval and Consent to Participate

Not applicable.

References

[1] Bechlioulis, C. P., & Rovithakis, G. A. (2011). Robust partial-state feedback prescribed performance control of cascade systems with unknown nonlinearities. *IEEE Transactions on Automatic Control*, *56*(9), 2224-2230. [CrossRef]

[2] Zhu, X., Chen, J., & Zhu, Z. H. (2021). Adaptive sliding mode disturbance observer-based control for rendezvous with non-cooperative spacecraft. *Acta Astronautica*, *183*, 59-74. [CrossRef]

[3] Guo, J., Pang, Z., & Du, Z. (2025). Combined trajectory and time-planning strategy for rendezvous missions using low-thrust transfer. *Astrodynamics*, *9*(4), 481-493. [CrossRef]

[4] Wang, J., Zhang, C., & Zhang, J. (2021). Analytical solution of satellite formation impulsive reconfiguration considering passive safety constraints. *Aerospace Science and Technology*, *119*, 107108. [CrossRef]

[5] Pavanello, Z., Pirovano, L., Armellin, R., De Vittori, A., & Di Lizia, P. (2025). Collision avoidance maneuver optimization during low-thrust propelled trajectories. *Astrodynamics*, *9*(2), 247-271. [CrossRef]

[6] Zhang, W., Zhao, Y., & Li, D. (2026). Disturbance-Free Payload spacecraft modeling and control: Non-contact architecture for high-precision space missions. *Astrodynamics*, 1-24. [CrossRef]

[7] Bechlioulis, C. P., Doulgeri, Z., & Rovithakis, G. A. (2012). Guaranteeing prescribed performance and contact maintenance via an approximation free robot force/position controller. *Automatica*, *48*(2), 360-365. [CrossRef]

[8] Shao, X., Hu, Q., Shi, Y., & Jiang, B. (2018). Fault-tolerant prescribed performance attitude tracking control for spacecraft under input saturation. *IEEE Transactions on Control Systems Technology*, *28*(2), 574-582. [CrossRef]

[9] Zhu, X., Chen, J., & Zhu, Z. H. (2021). Adaptive learning observer for spacecraft attitude control with actuator fault. *Aerospace Science and Technology*, *108*, 106389. [CrossRef]

[10] Sun, R., Shan, A., Zhang, C., Wu, J., & Jia, Q. (2021). Quantized fault-tolerant control for attitude stabilization with fixed-time disturbance observer. *Journal of Guidance, Control, and Dynamics*, *44*(2), 449-455. [CrossRef]

[11] Liu, C., Luo, Y., Lyu, B., & Shi, K. (2025). Observer-based dual hybrid nonfragile tracking control for satellite swarm reconstruction. *Astrodynamics*, *9*(5), 643-656. [CrossRef]

[12] Chen, J., Yu, Y., Zheng, Z., & Yuan, J. (2025). Distributed composite state observer-based cooperative control for spacecraft swarm. *Astrodynamics*, *9*(6), 821-835. [CrossRef]

[13] Shao, X., Hu, Q., & Shi, Y. (2020). Adaptive pose control for spacecraft proximity operations with prescribed performance under spatial motion constraints. *IEEE Transactions on Control Systems Technology*, *29*(4), 1405-1419. [CrossRef]

[14] Wei, C., Luo, J., Dai, H., & Duan, G. (2018). Learning-based adaptive attitude control of spacecraft formation with guaranteed prescribed performance. *IEEE transactions on cybernetics*, *49*(11), 4004-4016. [CrossRef]

[15] Shi, X. N., Chen, W., Li, R., Zhou, Z. G., & Wen, K. (2020, July). Prescribed Performance Attitude Tracking Control for Spacecraft under Multi-Constraint. In *2020 39th Chinese Control Conference* (CCC) (pp. 270-275). IEEE. [CrossRef]

[16] Liu, Y., Qin, K., Li, W., Shi, M., Lin, B., & Cao, L. (2022). Prescribed performance rotating formation control of multi-spacecraft systems with uncertainties. *Drones*, *6*(11), 348. [CrossRef]

[17] Yang, D., Yang, Y., Zong, G., & Sun, H. (2024). Prescribed performance adaptive fault-tolerant control for nonlinear systems with actuator faults and input dead-zone. *International Journal of Robust and Nonlinear Control*, *34*(9), 5949-5965. [CrossRef]

[18] Sun, R., Ahn, C. K., Liu, D., Wang, W., & Zhang, C. (2025). Near-asteroid spacecraft formation control with prescribed-performance: A dynamic event-triggered reinforcement learning control approach. *Aerospace Science and Technology*, *161*, 110138. [CrossRef]

[19] Zhang, W., Wang, Y., & Zhang, Y. (2025). Attention-driven reinforcement learning for multi-satellite collaborative orbital interception strategy solution. *Astrodynamics*, *9*(5), 657-669. [CrossRef]

[20] Holt, H., Baresi, N., & Armellin, R. (2024). Reinforced Lyapunov controllers for low-thrust lunar transfers. *Astrodynamics*, *8*(4), 633-656. [CrossRef]

[21] Li, B., Chen, M., Xia, J., Wu, J., & Guo, H. (2026). Switched Prescribed Performance-based Fault-Tolerant Attitude Tracking Control for Satellite. *IEEE Transactions on Automation Science and Engineering*. [CrossRef]

[22] Zhang, C., Lu, W., Zhao, S., Wu, J., Zhu, X., Liu, Z., & He, W. (2025). Enhancing Attitude Tracking With Self-Learning Control Using Tanh-Type Learning Intensity. *IEEE Transactions on Automation Science and Engineering*, *22*, 16976-16986. [CrossRef]

[23] Zhang, C., Xiao, B., Wu, J., & Li, B. (2021). On low-complexity control design to spacecraft attitude stabilization: An online-learning approach. *Aerospace Science and Technology*, *110*, 106441. [CrossRef]

[24] Zhang, C., Ma, G., Sun, Y., & Li, C. (2019). Observer-based prescribed performance attitude control for flexible spacecraft with actuator saturation. *ISA transactions*, *89*, 84-95. [CrossRef]

[25] Ma, G., Wu, H., Zhao, Z., Zou, T., & Hong, K.-S. (2022). Adaptive neural network control of a non-linear two-degree-of-freedom helicopter system with prescribed performance. *IET Control Theory & Applications*, *17*(13), 1789-1799. [CrossRef]

[26] Mu, Q., Long, F., & Li, B. (2023). Adaptive neural network prescribed performance control for dual switching nonlinear time-delay system. *Scientific Reports*, *13*(1), 8132. [CrossRef]

[27] Xu, L. X., Wang, Y. L., Wang, X., & Peng, C. (2022). Decentralized event-triggered adaptive control for interconnected nonlinear systems with actuator failures. *IEEE Transactions on Fuzzy Systems*, *31*(1), 148-159. [CrossRef]

[28] Bu, X., Lv, M., Lei, H., & Cao, J. (2023). Fuzzy Neural Pseudo Control With Prescribed Performance for Waverider Vehicles: A Fragility-Avoidance Approach. *IEEE Transactions on Cybernetics*, *53*(8), 4986-4999. [CrossRef]

[29] Han, S. I., & Lee, J. M. (2013). Improved prescribed performance constraint control for a strict feedback non-linear dynamic system. *IET Control Theory & Applications*, *7*(14), 1818-1827. [CrossRef]

[30] Bu, X., Wu, X., Zhu, F., Huang, J., Ma, Z., & Zhang, R. (2015). Novel prescribed performance neural control of a flexible air-breathing hypersonic vehicle with unknown initial errors. *ISA transactions*, *59*, 149-159. [CrossRef]

[31] Lei, J., Meng, T., Wang, W., Li, H., & Jin, Z. (2023). Singularity-Avoidance Prescribed Performance Control for Spacecraft Attitude Tracking. *IEEE Transactions on Aerospace and Electronic Systems*, *59*(5), 5405-5421. [CrossRef]

[32] Liu, Q., Zhang, K., & Jiang, B. (2022). Fixed-time fault estimation and prescribed performance fault-tolerant control for interconnected systems. *IEEE Transactions on Cybernetics*, *54*(2), 1084-1095. [CrossRef]

[33] Bu, X., Jiang, B., & Lei, H. (2022). Nonfragile quantitative prescribed performance control of waverider vehicles with actuator saturation. *IEEE Transactions on Aerospace and Electronic Systems*, *58*(4), 3538-3548. [CrossRef]

[34] Mehdifar, F., Bechlioulis, C. P., Hashemzadeh, F., & Baradarannia, M. (2020). Prescribed performance distance-based formation control of multi-agent systems. *Automatica*, *119*, 109086. [CrossRef]

[35] Rodrigues, V. H. P., Hsu, L., Oliveira, T. R., & Fridman, L. (2022). Adaptive sliding mode control with guaranteed performance based on monitoring and barrier functions. *International Journal of Adaptive Control and Signal Processing*, *36*(6), 1252-1271. [CrossRef]

[36] Obeid, H., Fridman, L. M., Laghrouche, S., & Harmouche, M. (2018). Barrier function-based adaptive sliding mode control. *Automatica*, *93*, 540-544. [CrossRef]

[37] Cruz-Ancona, C. D., Fridman, L., Obeid, H., Laghrouche, S., & Pérez-Pinacho, C. A. (2023). A uniform reaching phase strategy in adaptive sliding mode control. *Automatica*, *150*, 110854. [CrossRef]

[38] Laghrouche, S., Harmouche, M., Chitour, Y., Obeid,

H., & Fridman, L. M. (2021). Barrier function-based adaptive higher order sliding mode controllers. *Automatica*, *123*, 109355. [CrossRef]

[39] Obeid, H., Laghrouche, S., Fridman, L., Chitour, Y., & Harmouche, M. (2020). Barrier function-based adaptive super-twisting controller. *IEEE Transactions on Automatic Control*, *65*(11), 4928-4933. [CrossRef]

[40] Zhao, Z., Wu, J., Liu, Z., He, W., & Chen, C. P. (2024). Adaptive neural network control of a 2-DOF helicopter system considering input constraints and global prescribed performance. *Science China Information Sciences*, *67*(7), 172202. [CrossRef]

[41] Zhao, Z., Zhang, J., Liu, Z., Li, H. X., & Chen, C. P. (2024). Event-triggered adaptive neural fault-tolerant control for a 2-DOF helicopter system with prescribed performance. *Automatica*, *162*, 111511. [CrossRef]

[42] Wu, B. (2016). Spacecraft attitude control with input quantization. *Journal of Guidance, Control, and Dynamics*, *39*(1), 176-181. [CrossRef]

[43] Utkin, V. (2013). On convergence time and disturbance rejection of super-twisting control. *IEEE Transactions on Automatic Control*, *58*(8), 2013-2017. [CrossRef]

[44] Kim, S.-K., & Ahn, C. K. (2021). Performance-boosting attitude control for 2-DOF helicopter applications via surface stabilization approach. *IEEE Transactions on Industrial Electronics*, *69*(7), 7234-7243. [CrossRef]

Xiaoyu Zhu received the Ph.D. degrees in control science and engineering from the Department of Aerospace Information and Control, Shanghai Jiao Tong University, Shanghai, China, in 2021. He is currently a Postdoctoral Researcher with the School of Aeronautics and Astronautics, Shanghai Jiao Tong University, Shanghai, China. His research interests include spacecraft control, autonomous rendezvous, and prescribed performance control.

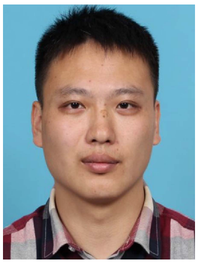

Ran Sun received the M.S. and Ph.D. degrees in control science and engineering from the Department of Aerospace Information and Control, Shanghai Jiao Tong University, Shanghai, China, in 2019. He is currently a Postdoctoral Researcher with the School of Aeronautics and Astronautics, Shanghai Jiao Tong University, Shanghai, China. His research interests include formation flying, nonlinear control, and reinforcement learning.

Jihe Wang received the bachelor's degree in aircraft design from the Harbin Institute of Technology, Harbin, China, in 2005, and the Ph.D. degree in aerospace science and technology from the University of Tokyo, Tokyo, Japan, in 2012. He is currently an Associate Professor with the School of Aeronautics and Astronautics, Sun Yat-Sen University (Shenzhen Campus), Shenzhen 518107, China. He participated in more than ten projects, including 863, 973, high-level special subprojects, the National Natural Science Foundation of China, and National Defense pre-research projects. His research interests include spacecraft dynamics and control research, including formation/cluster dynamics and control, spacecraft drag-free control, ground numerical, and semi-physical simulation of multiple spacecraft systems.

Pukun Lu was born in Changchun City, China. He is currently working toward Ph.D. degree in control theory and control engineering from Northeast Electric Power University, Jilin.

He is currently an International Visiting Research Trainee with the Department of Earth and Space Science and Engineering, York University, Toronto, ON, Canada. His research interests include robust and adaptive control for nonlinear systems.